Journal of Insect Physiology 95 (2016) 118–132

Contents lists available at ScienceDirect

Journal of Insect Physiology

journal homepage: www.elsevier.com/locate/jinsphys

Lipogenesis in a wing-polymorphic cricket: Canalization versus morph-specific plasticity as a function of nutritional heterogeneity

Anthony J. Zera [a,*], Rebecca Clark [a], Spencer T. Behmer [b]

[a] School of Biological Sciences, University of Nebraska, Lincoln, NE 68588, United States
[b] Department of Entomology, Texas A&M University, College Station, TX 77843, United States

ARTICLE INFO

Article history:
Received 27 June 2016
Received in revised form 22 September 2016
Accepted 25 September 2016
Available online 28 September 2016

ABSTRACT

The influence of variable nutritional input on life history adaptation is a central, but incompletely understood aspect of life history physiology. The wing-polymorphic cricket, *Gryllus firmus,* has been extensively studied with respect to the biochemical basis of life history adaptation, in particular, modification of lipid metabolism that underlies the enhanced accumulation of lipid flight fuel in the dispersing morph [LW(f) = long wings with functional flight muscles] relative to the flightless (SW = short-winged) morph. To date, biochemical studies have been undertaken almost exclusively using a single laboratory diet. Thus, the extent to which nutritional heterogeneity, likely experienced in the field, influences this key morph adaptation is unknown. We used the experimental approach of the Geometric Framework for Nutrition and employed 13 diets that differed in the amounts and ratios of protein and carbohydrate to assess how nutrient amount and balance affects morph-specific lipid biosynthesis. Greater lipid biosynthesis and allocation to the soma in the LW(f) compared with the SW morph (1) occurred across the entire protein-carbohydrate landscape and (2) is likely an important contributor to elevated somatic lipid in the LW(f) morph across the entire protein-carbohydrate landscape. Nevertheless, dietary carbohydrate strongly affected lipid biosynthesis in a morph-specific manner (to a greater degree in the LW(f) morph). Lipogenesis in the SW morph may be constrained due to its more limited lipid storage capacity compared to the LW(f) morph. Elevated activity of $NADP^+$-isocitrate dehydrogenase ($NADP^+$-IDH), an enzyme that produces reducing equivalents for lipid biosynthesis, was correlated with and may be an important cause of the increased lipogenesis in the LW(f) morph across most, but not all regions of the protein-carbohydrate landscape. By contrast, ATP-citrate lyase (ACL), an enzyme that catalyzes the first step in the pathway of fatty acid biosynthesis, showed complex morph-specific patterns of activity that were strongly contingent upon diet. Morph-specific patterns of $NADP^+$-IDH and ACL activities across the nutrient landscape were much more complex than expected from previous studies on a single diet. Collectively, our results indicate that the biochemical basis of an important life history adaptation, morph-specific lipogenesis, can be canalized in the face of substantial nutritional heterogeneity. However, in some regions of the protein-carbohydrate landscape, it is strongly modulated in a morph-specific manner.

1. Introduction

Wing polymorphism is a common feature of insects, consisting of flight-capable and flightless morphs within the same population that are adapted for dispersal at the expense of reproductive output, and vice versa (Harrison, 1980; Zera and Denno, 1997; Guerra, 2011; Zera and Brisson, 2012). The polymorphism has been extensively studied from ecological, behavioral, physiological, biochemical, and molecular perspectives to understand the functional basis of morph adaptation for dispersal versus reproduction. It has also served as a major experimental model in functional studies of life history trade-offs, a central topic in life history evolution (see above references).

Physiological and biochemical aspects of the polymorphism have been especially well-studied in the wing-dimorphic cricket, *Gryllus firmus* (reviewed in Zera, 2005, 2009; Zera and Harshman, 2011; Schilder et al., 2011; Vellichirammal et al., 2014). This species consists of a flight-capable morph with fully developed wings and flight muscles [LW(f) = long wings and functional flight muscles] and an obligately flightless morph that does not fully develop wings or flight muscles and which cannot fly (SW = short-winged). A key difference between the morphs is the significantly greater accumulation of lipid (main flight fuel) by the LW(f) morph during

* Corresponding author.
E-mail address: azera1@unl.edu (A.J. Zera).

http://dx.doi.org/10.1016/j.jinsphys.2016.09.015
0022-1910/

adulthood. This is due to elevated expression of genes and activities of lipogenic enzymes that result in elevated flux through the pathways of fatty-acid and triglyceride biosynthesis in LW(f) adults (Zhao and Zera, 2002; Zera and Zhao, 2003; Zera 2005; Zera and Harshman, 2011; Vellichirammal et al., 2014). Importantly, reduced lipid production in the SW morph allows this morph to allocate a greater proportion of ingested nutrients (e.g., protein and carbohydrates) to egg production, accounting, at least in part, for its substantially elevated fecundity, relative to the LW(f) morph (see above references).

Despite considerable study, many important aspects of morph-specific lipid metabolism have yet to be investigated in *G. firmus* morphs. One potentially-important, but neglected, aspect is how variable food nutritional input influences morph-specific lipid biosynthesis and its trade-off with egg production. The role of variable nutrient acquisition on life history trade-offs is a long-standing issue that has become an increasingly important focus of life history physiology (van Noordwijk and de Jong, 1986; Zera and Harshman, 2001; Lee et al., 2008; Boggs, 2009; Flatt and Heyland, 2011; Musselman et al., 2013). To date, nearly all previous physiological, biochemical and molecular studies of lipid metabolism in *G. firmus* have been conducted on a single diet, or in a limited number of studies, the total nutrient content of a single diet was altered (e.g. reduced by 50–75%; e.g. Zhao and Zera, 2002; Zera and Zhao, 2003, 2006; Zera and Harshman, 2011). Thus, we currently have a very narrow understanding of the effects of food nutrient content on the biochemical basis of life history specialization and trade-offs.

One effective way to investigate the influence of food nutritional heterogeneity on various organismal functions is to employ the experimental approach of the Geometric Framework for Nutrition (Simpson and Raubenheimer, 1999, 2012; Behmer, 2009). In essence, this approach examines animal responses over a range of foods that differ in specific nutrients. Typically protein and carbohydrate content are the nutrients that are manipulated because they have very strong effects on growth and reproduction, and are actively regulated by most animals, including insects (Behmer, 2009). Response variables (e.g., consumption, respiration, lipid accumulation, various life history traits) are then measured as a function of food protein-carbohydrate content. Because a relatively large number of diets are often used in these studies (e.g., 13 in the present study; see below), quantitative effects of variation in food protein and carbohydrate amounts and balance, as well as total caloric content, can be assessed. This experimental approach thus overcomes many of the limitations of previous studies of life history nutritional physiology, in which the nutritional environment (i.e., variation in diet) has not been well quantified or controlled, and where the nutrient space was severely restricted because only a few diets were used (Lee et al., 2008; and references therein).

We recently demonstrated, using the experimental approach of the Geometric Framework, that LW(f) adult *G. firmus* females have significantly greater somatic lipid content than SW females over a wide protein-carbohydrate landscape, involving diets that differ in carbohydrate and protein (see Discussion, and Clark et al. (2015)). This result extended our previous findings of greater somatic lipid in LW(f) vs. SW females fed a single diet. However, the underlying biochemical causes for this finding were unknown. In the present study we reared flight-capable adult female morphs of *Gryllus firmus* on a wide range of diets that differed in their protein-carbohydrate content, and then quantified key aspects of lipid biosynthesis and allocation to somatic and reproductive body compartments. Specifically, we measured the rate of whole-organism lipid biosynthesis – using a radiolabeled lipid precursor (^{14}C-acetate) – and allocation of biosynthesized lipid to somatic and ovarian body compartments in LW(f) and SW adult females. In addition, we quantified specific activities of two important lipogenic enzymes: (1) $NADP^+$-isocitrate dehydrogenase ($NADP^+$-IDH), which is an important contributor of reduced NADPH required for lipogenesis and (2) ATP-citrate lyase (ACL), which catalyzes the first step in the *de novo* pathway of fatty acid biosynthesis (Zera, 2005). Activities of these two enzymes are strongly and positively correlated genetically with each other, with activities of three other lipogenic enzymes, and with rate of lipid biosynthesis in wing morphs of *G. firmus* fed the standard laboratory diet (Zera and Zhao, 2003; Zera, 2005). The present study used 13 precisely defined diets that varied in the total amount and balance of protein and carbohydrate content. This array of diets allowed us to investigate how the magnitude of morph-specific variation in lipid biosynthesis and ovarian growth, and their trade-off, varied across a broad protein-carbohydrate landscape.

2. Methods

2.1. Crickets and diets

Gryllus firmus females used in the present study were derived from two large outbred laboratory populations: one population primarily (>90%) produces the flight-capable morph with long wings and fully developed flight muscles [LW(f)], while the other primarily (>95%) produces the SW flightless morph with shortened nonfunctional wings and underdeveloped non-functional flight muscles. Some LW(f) individuals are transformed into a flightless morph during adulthood due to histolysis of flight muscles [denoted as the LW(h) morph; Zera, 2009]. This morph, which has reproductive, physiological, and biochemical characteristics more similar to SW females than LW(f) females (Zera, 2009), is not considered in the present study. Our *Gryllus firmus* populations were founded from individuals collected at Gainesville, Florida in the mid-1990s and have been maintained since then in the laboratory under a 16 light: 8 dark photo regime, at 28 °C and fed a standard laboratory diet (Zera, 2005). Each population was propagated each generation by breeding 100–250 individuals. These populations, which are part of a larger group of populations produced by artificial selection, are the same as those investigated previously in numerous biochemical and physiological studies of morph adaptation (e.g. Zera and Larsen, 2001; Zhao and Zera, 2002; Zera and Zhao 2003, 2006; reviewed in Zera and Harshman, 2011). Although only one pair of LW(f) and SW lines was investigated in the present study, previous studies have shown that biochemical and reproductive differences between any pair of LW(f) and SW lines are typically very similar to differences between of other LW(f) and SW lines (see above references). Biochemical data analogous to those reported here will be reported for the other LW(f) and SW selected lines in forthcoming papers. Additional information on these populations can be found in references cited above.

Individuals that had molted into adults during the previous 24 h were transferred from the standard laboratory diet to plastic boxes ($14'' \times 9'' \times 6''$; 6–12 crickets per box) that contained one of 13 chemically-defined diets that differed in protein (p) or carbohydrate (c) content (see Appendix 1, and Clark et al. (2015) for information on diet composition). Previous work has shown that these crickets self-select a protein-to-carbohydrate ratio of p3:c4; this "balanced" ratio was used along with two ratios that were protein-biased (p17.25:c14.25 and p14:c7) and two ratios that were carbohydrate-biased (p4:c17 and p9.75:c21.75; Clark et al., 2013). In addition, for each p:c ratio, two or three total macronutrient contents were used, so that total diet macronutrient content ranged from dilute (21% total macronutrients) to concentrated (63%). Food was placed in plastic dishes and was continually replenished during the experiment (see Clark et al., 2013). Boxes also contained two 50 mL cotton-plugged plastic vials containing

water. Both LW(f) and SW females were raised in the same box. Boxes were kept at 28 °C, 16L:8D for five days at which point crickets were weighed and injected with radiolabeled [1-^{14}C] Na-acetate as described below. In a few instances, a cricket was cannibalized during the 5-day period prior to injection. Where this occurred the remaining crickets in that box were eliminated from the study.

2.2. Quantification of whole body lipid biosynthesis

Incorporation of radiolabelled [1-^{14}C] Na- acetate into lipid was performed essentially as in Zhao and Zera (2001, 2002), with a few slight modifications. Briefly, about 800,000–900,000 DPM of [1-^{14}C] Na-acetate (2.0 Gbq/mmol; 54.7 mCi/mmol) in 3 µl of 0.9% NaCl solution were injected in the abdominal hemocoel of a cricket. Injections were performed within 2–4 h after lights on, in crickets that had been starved for 2 h prior to injection. Any hemolymph that bled at the site of injection was wiped with a small piece of adsorbent paper; radioactivity on this paper was quantified by liquid scintillation spectrometry, and subtracted from DPM injected. Each day, DPM in three replicates of the injection solution were also determined so that percent incorporation of radiolabel into lipid could be calculated. After injection, crickets were placed singly in 16 oz (ca 500 mL) plastic cups and kept at 28 °C 16L:8D for 3 h (this was within the linear range of incorporation of radiolabel into total lipid versus time (see Fig 1 of Zhao and Zera (2001)). After the incubation period, crickets were quickly frozen at −86 °C.

Crickets were subsequently thawed and weighed, flight muscle status scored (pink or white), and ovaries removed and weighed. Flight muscle status was recorded because, as mentioned previously, some LW(f) individuals histolyze their flight muscles and become flightless; results for LW(h) females will be reported elsewhere. To determine how much radiolabel was incorporated into somatic and reproductive tissues, ovaries were removed and placed in 1.5 mL Eppendorf tubes, to which were added 500 µL of chloroform/methanol (2:1 v/v). Cricket bodies without ovaries were placed individually in glass tubes, to which were added 5 mL of chloroform/methanol (2:1, v/v). Tubes containing ovaries or cricket bodies were stored at −20 °C until lipid extraction. Bodies were homogenized for 2 min with a glass rod attached to an electric motor, and the mixture was filtered through Whatman #1 paper. The residue was returned to the tube and the process was repeated. The total chloroform/methanol extract was washed with ¼ of its volume with 0.88% aqueous KCl, followed by two additional washes of 0.88% KCl in water (1/8th of extract volume) and methanol (1:1, v/v; 1/8th of extract volume). These washes were done to remove unreacted radiolabeled Na-acetate as well

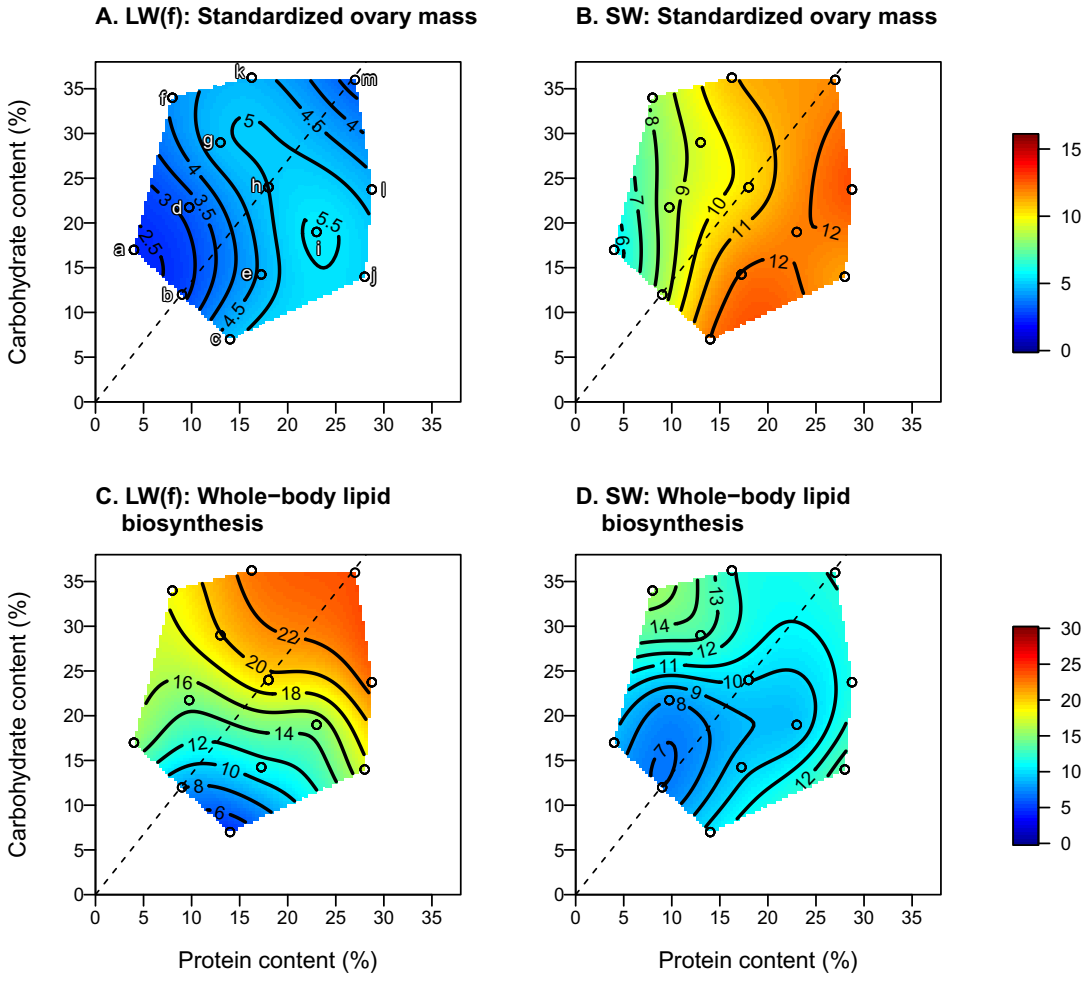

Fig. 1. Response surfaces of standardized ovarian masses and whole-body lipid biosynthesis for both morphs. Data (means ± SEM) for the LW(f) morphs are shown in panels (A) and (C); SW morphs are shown in panels (B) and (D). Measurements were made on day-5 of adulthood in BK-2 LW(f) and SW selected lines. Standardized ovarian masses were calculated as ovarian wet mass divided by whole-body wet mass. Response surfaces of absolute ovarian mass are virtually identical to those of standardized ovarian mass. Rate of whole body lipid biosynthesis = percentage of injected radiolabeled ^{14}C-Na-acetate incorporated into total lipid over a four hour incubation period. See Methods for additional details.

as contaminating chloroform-soluble carbohydrates. The volume of the washed chloroform/methanol solution was reduced to 3 mL, 2.7 mL of which were placed in scintillation vials. The solutions were evaporated to dryness on a heating block, three mL of scintillation cocktail were added, the tubes were kept in the dark overnight to reduce chemiluminescence, and DPM quantified the next day. Ovarian lipids were extracted in a similar way as somatic lipid, except that ovaries in chloroform/methanol were sonicated for ten seconds, centrifuged at 13,000×*g*, and organic solvent removed. This process was repeated, the extracts were combined and washed with aqueous KCl, and the lower organic phase was removed and counted as described above. DPM incorporated into total lipid were divided by total DPM injected to obtain% injected radiolabel incorporated into lipid.

2.3. Quantification of enzyme activities

Fat body specific activities of $NADP^+$-isocitrate dehydrogenase ($NADP^+$-IDH; E.C. 1.1.1.42) and ATP-citrate lyase (E.C. 4.1.3.8) were measured using standard spectrophotometric assay procedures

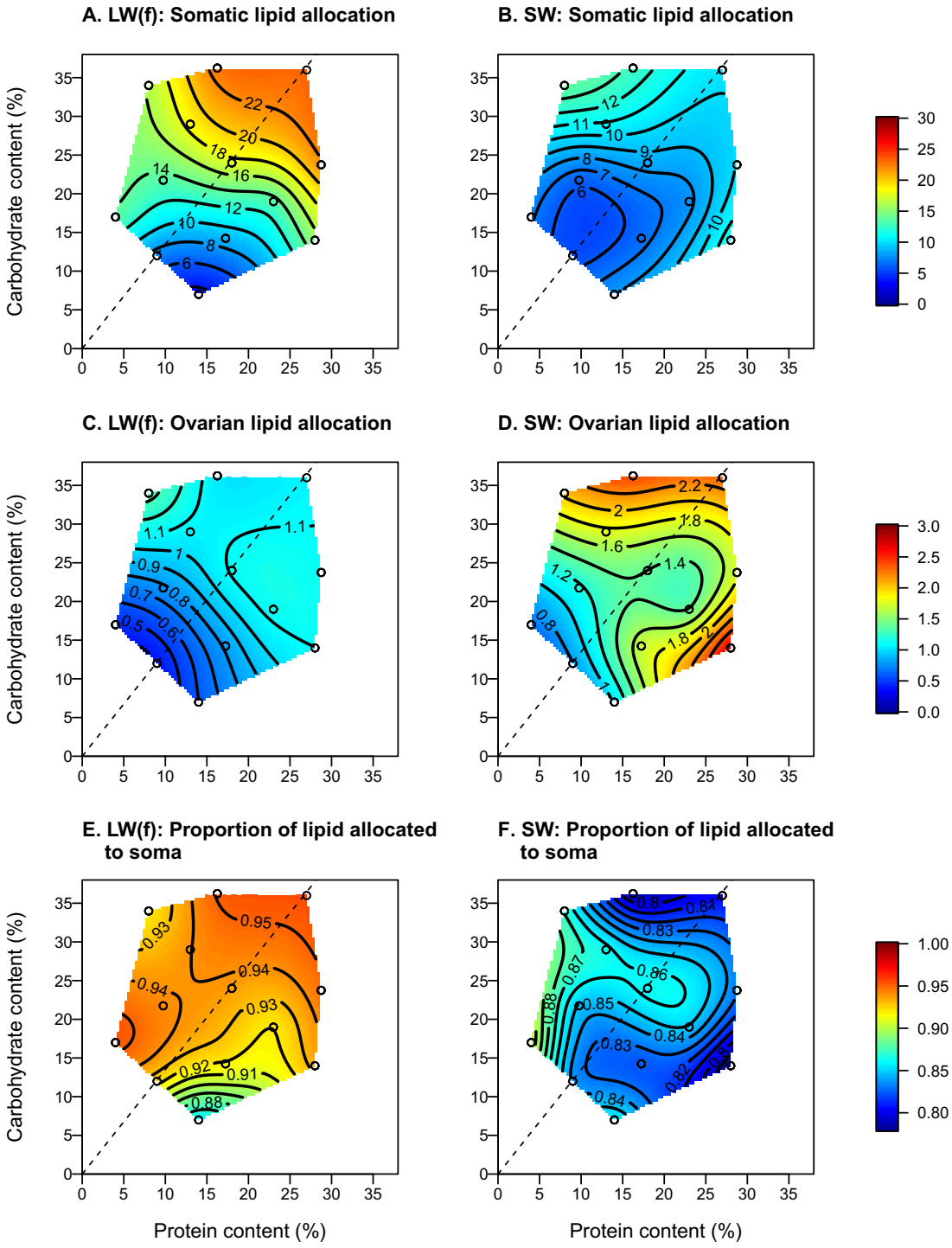

Fig. 2. Response surfaces of biosynthesized lipid allocated to the soma, to the ovaries, and as a proportion allocated to the soma (whole body minus ovaries). Data (means ± SEM) for LW(f) morphs are shown in panels (A), (C) and (E); SW morphs are shown in panels (B), (D) and (F). Allocation is the percentage of radiobiosynthesized total lipid measured in Fig 1 that was found in the soma or ovaries.

described previously (Zhao and Zera, 2001; Zera and Zhao, 2003), with a few modifications. Enzymes activities were measured on a different group of crickets from those used to measure lipid biosynthetic rates but which were fed the same diets and raised under the same conditions. Briefly, on day 5 of adulthood, after the feeding trial, 10–30 mg of fat body were removed and homogenized in 50 mM K^+-phosphate buffer (pH 7.4), containing 0.1% β-mercaptoethanol, 5 mM ethylenediaminetetraacetic acid (EDTA) and 10% glycerol. Enzyme homogenate was further diluted with homogenizing buffer but without glycerol for reasons described below. Eight μL of diluted homogenate was added to 192 μL of enzyme cocktail described in Zhao and Zera (2001). Change in absorbance at 340 nm was measured for six minutes after one min incubation at 28 °C in a Fluorostar Omega spectrophotometer. Previous studies had shown that six minutes was within the "linear" period of the progress curve and that the enzyme dilutions used resulted in activities that were linear with respect to enzyme concentration; both preconditions are needed for steady-state kinetic analysis. Protein concentrations of homogenates were measured using the Bradford protein assay with bovine serum albumen as the standard (Stoscheck, 1990).

2.4. Statistical analyses and response surfaces

General linear models performed in R (version 2.15.3) were used to analyze biochemical and reproductive characteristics as a function of % carbohydrate and % protein in the diet. In the present study, we were mainly interested in assessing morph differences in response variables (e.g. % incorporation of radiolabel into lipid, enzyme specific activity, ovarian weight) as a function of diet macronutrients (% carbohydrate and % protein). The overall difference between the LW(f) and SW morphs for a particular variable was assessed by a partial F-test in which the full statistical model containing all morph and macronutrient terms (main effects of morph, protein and carbohydrate, as well as eight interaction terms) was compared with a reduced model without any morph terms (see below and Clark et al. (2015, 2016)). A significant difference between the two models was interpreted as a significant overall effect of morph. Results of the analyses of the full model containing all morph, protein, and carbohydrate main effects and interaction terms are reported because these results illustrate the nature of the morph differences. In one case (ovarian lipid biosynthesis), no significant effect of morph was found and thus results of the reduced model without morph terms are reported. This reduced analysis is included as it assesses effects of macronutrients independent of morph on response variables. In these analyses, macronutrient axes were standardized using the rsm package (Lenth, 2009).

Variation in each response variable for each morph is presented as a non-parametric response surface figure. These surfaces provide a more detailed visualization of the experimental data as compared with graphing the best-fitting response surface regression models. These non-parametric response surface figures were generated with the thin-plate splines function (Tps) from the "fields" package in R (Furrer et al., 2012), using lambda set equal to 0.01. However, response surface figures only provide a qualitative measure of morph-specific variation in response variables. Thus, quantitative differences between separate morph-specific response surfaces were assessed by statistical comparisons of the estimated linear and quadratic terms for diet protein and carbohydrate content, as well as protein × carbohydrate interaction term(s). A significant and negative quadratic term (i.e. protein × protein or carbohydrate × carbohydrate) indicates that the response surface is curved in that dimension, and that an intermediate amount of nutrient produces a maximal response. In contrast, if only linear model terms are significant, the response surface shape is flat, and maximal and minimal responses occur at edges of the response surface. Significant protein × carbohydrate interaction terms indicate that the response surface shape is complex, and response characteristics will depend on specific combinations of protein and carbohydrate for each morph.

3. Results

Means ± SEMs of each response variable for each morph on each diet, which were used to construct the response surfaces, are given in Appendix 2. Summary of the statistical analyses of these data are given in Table 1, while the full results of analyses are given in Appendix 3.

3.1. Ovarian masses

At the end of the 5-day feeding trial, ovarian wet mass standardized to whole-body wet mass (%) was substantially larger for the SW morph compared with the LW(f) morph over the entire protein-carbohydrate landscape: Morph means (±SEM): LW(f): 4.4 ± 0.3%; SW: 10.3 ± 0.5%; Fig 1A, B; partial F-test of models with (=full) and without (=reduced) "morph": $F_{6,126} = 15.4$, $P < 0.001$, Table 1, Appendix 3A). Ovarian mass differed between morphs ($F_{1,126} = 128.1$, $P < 0.001$), and there was a significant morph × protein interaction ($F_{1,126} = 5.6$, $P = 0.02$). This interaction was due to increasing ovarian mass in the SW morph with increasing diet protein content (Fig 1B), which resulted in a significant linear protein coefficient: 22.8 ± 6.7; $P < 0.05$, Table 2. By contrast, the LW (f) morph exhibited smaller ovaries that were nearly invariant across the entire protein-carbohydrate landscape (Fig 1A).

3.2. Whole-body lipid biosynthesis

Across all diets, percent incorporation of ^{14}C-acetate into whole-body lipid during the three h incubation period was substantially (ca. 50%) higher in the LW(f) compared to the SW morph [LW(f) = 16.5 ± 0.95%, N = 53; SW = 10.9 ± 0.90%, N = 56; Partial F-test of full vs. reduced models: $F_{6,96} = 5.74$, $P < 0.001$; Fig. 1C, D; Table 1; Appendix 3B]. This is evident by the much higher incorporation values across nearly the entire protein-carbohydrate landscape for the LW(f) morph (Fig 1C, D).

Of the two main macronutrients in the diet, carbohydrate strongly and positively affected lipid biosynthesis ($F_{1,96} = 20.6$; $P < 0.0001$, Appendix 3B), while protein content had no observed effect. This is clearly seen in the response surface graphs (Fig 1C, D) in which rate of lipid biosynthesis increased linearly (i.e. vertically) with dietary carbohydrate for each morph.

In addition to these main effects, a highly significant morph × carbohydrate interaction on the rate of whole-body lipid biosynthesis was also observed ($F_{1,96} = 7.24$, $P = 0.008$; Table 1; Appendix 3B). This is evident qualitatively by the much greater increase in the rate of lipid biosynthesis with increasing dietary carbohydrate in the LW(f) morph compared with the SW morph (Fig 1C, D), and quantitatively by the highly significant linear coefficient for the effect of carbohydrate on the response surface (Table 2) for the LW(f) morph (7.66 ± 1.20, $P < 0.05$) but not the SW morph (1.62 ± 1.27, ns). Finally, there was a significant protein × carbohydrate interaction for the SW but not the LW(f) morph (protein × carbohydrate coefficient for the SW morph = −4.72 + 2.35, $P < 0.05$, Table 2). This was evident by the increased rate of lipid biosynthesis on two opposing edges of the response surface corresponding to high protein and low carbohydrate diets, but vice versa for the SW morph (Fig 1C, D). In summary, there was an overall higher rate of whole-body lipid biosynthesis for the LW(f) compared to the SW morph across the

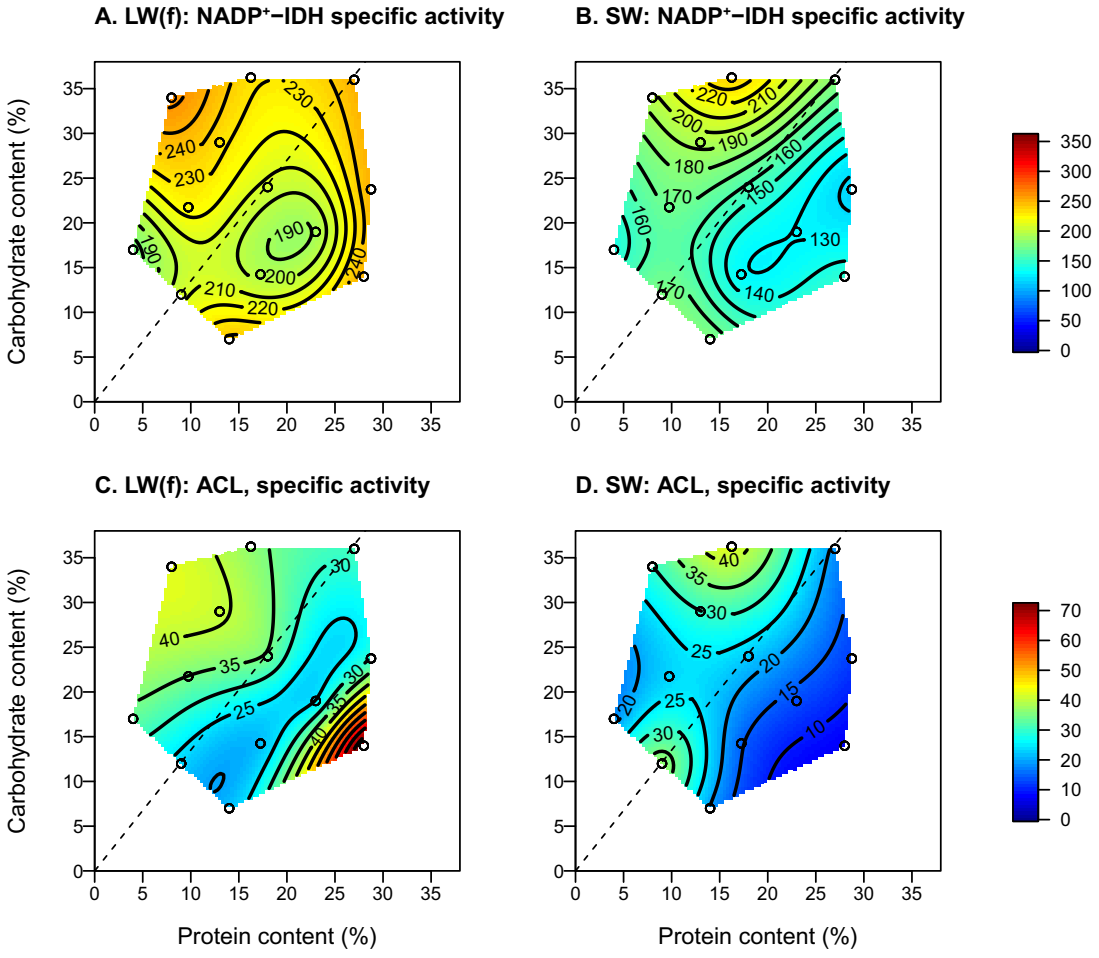

Fig. 3. Response surfaces of enzymatic specific activities associated with lipogenesis. Data (mean (nmol/min/mg protein)±SEM) for fat body NADP$^+$-isocitrate dehydrogenase (NADP$^+$-IDH) [LW(f) morph = panel A; SW morph = panel B], and ATP-citrate lyase (ACL) [LW(f) morph = panel C; SW morph = panel D].

Table 1
Summary of result of ANCOVAs of response surface models testing the effects of protein and carbohydrate concentration, and morph type [SW vs. LW(f)], on aspects of lipid biosynthesis and ovarian mass. Initial cricket mass was included in models as a covariate, and protein and carbohydrate model terms were standardized to a scale from −1 to 1. *** = P < 0.001; ** = P < 0.01; * = P < 0.05; B = borderline, 0.1 > P < 0.05. Full results of the statistical analyses are given in Appendix 3A–G.

Model terms	Whole-body lipid biosynthesis	Somatic lipid allocation	Ovarian lipid allocation	Relative allocation to soma	NADP$^+$IDH specific activity	ACL specific activity	Ovarian Mass (total mass covariate)
Full model	***	***	***	***	***	***	***
Intercept	B	*	***	***	***	***	***
Initial cricket mass (covariate)	NS	NS					***
Morph	**	***	NS	**	*	NS	***
Protein	NS	*	NS	NS	NS	NS	NS
Carbohydrate	***	***	NS	NS	NS	NS	NS
Protein × Protein	NS	NS	NS	NS	NS	**	NS
Carbohydrate × Carbohydrate	NS	NS	NS	NS	NS	NS	NS
Protein × Carbohydrate	NS	NS	NS	NS	B	***	NS
Morph × Protein	NS	NS	NS	NS	B	*	**
Morph × Carbohydrate	**	**	NS	NS	NS	NS	NS
Morph × Protein^2	NS	NS	NS	NS	NS	**	NS
Morph × Carbohydrate^2	*NS*	*	NS	NS	NS	NS	NS
Morph × Protein × Carbohydrate	NS	*B*	NS	NS	NS	**	NS
Model adjusted R^2	0.31	0.37	0.24	0.28	.29	.21	.61
Morph differences: Partial F-test between models with/without 6 "Morph" terms	***	***	**	***	***	***	***

entire protein-carbohydrate landscape, and the magnitude of the difference between the morphs also varied across the landscape mainly as a function of carbohydrate content of the diet. Near the very bottom of the response surface graph (lowest carbohydrate diets), rate of lipid biosynthesis was the lowest for each morph and the least different between morphs.

Table 2
Coefficients (β ± s.e.m.) indicating the magnitude and significance of linear and quadratic aspects of response surfaces of ovary masses and whole body lipid biosynthesis of LW(f) and SW morphs presented in Fig. 1.

Model terms	Ovary mass		Whole body lipid biosynthesis	
Morph	LW(f)	SW	LW(f)	SW
Intercept	**−84.20 ± 19.31**	*−63.39 ± 33.38*	8.13 ± 8.99	2.21 ± 6.18
Initial cricket mass (covariate)	**0.15 ± 0.02**	**0.18 ± 0.04**	0.01 ± 0.01	0.01 ± 0.01
Protein	4.01 ± 4.28	**22.78 ± 6.73**	2.03 ± 1.89	0.25 ± 1.32
Carbohydrate	−6.69 ± 4.74	−7.37 ± 6.61	**7.66 ± 1.20**	1.62 ± 1.27
Protein × Protein	−7.60 ± 6.90	−15.53 ± 11.20	4.20 ± 3.16	2.51 ± 2.22
Carbohydrate × Carbohydrate	0.50 ± 7.96	4.99 ± 12.33	−3.74 ± 3.43	3.13 ± 2.36
Protein × Carbohydrate	−14.04 ± 8.84	7.15 ± 12.65	*0.22 ± 3.56*	**−4.72 ± 2.35**
R^2 (adjusted)	0.43	0.39	0.27	0.11
Model significance	**$F_{6,62}$ = 9.69, *P* < 0.001**	**$F_{6,63}$ = 8.25, *P* < 0.001**	***$F_{6,46}$ = 4.18, P = 0.002***	$F_{6,49}$ = 2.11 P = 0.07

Coefficients were estimated using general linear models. Protein and carbohydrate model terms were standardized to a scale from −1 to 1. Terms in bold are significant at the α < 0.05 level, and italicized terms are borderline significant (α < 0.10). Negative quadratic regression coefficients indicate a peak (convex) relationship, whereas positive quadratic regression coefficients indicate a trough (concave) relationship. The most inclusive models are presented to facilitate comparisons between the morphs. See Materials and Methods for explanations of "linear" and "quadratic" coefficients.

3.3. Somatic lipid allocation

Radiobiosynthesized lipid found in the soma (whole body minus ovaries) was significantly higher in the LW(f) morph (14.9 ± 0.80%; N = 68) compared with the SW morph (9.10 ± 0.73; N = 69; partial F-test of full and reduced models: $F_{6,124}$ = 8.23, P < 0.001; Table 1; Appendix 3C; Fig 2A, B). As was the case for total lipid biosynthesis, carbohydrate content of the diet also affected the amount of radiolabel incorporated into somatic lipid ($F_{1,124}$ = 35.6, P < 0.0001), and there was a strong morph × carbohydrate interaction ($F_{1,124}$ = 11.13, P = 0.001). Significant linear coefficients for the effect of carbohydrate on the separate morph response surfaces were observed for both the LW(f) (8.34 ± 1.65, P < 0.05) and SW morphs (2.26 ± 1.04, P < 0.05; Table 3) indicating a positive effect of carbohydrate on the amount of somatic lipid produced. The effect of carbohydrate was four times stronger in the LW(f) morph, thus giving rise to the morph × carbohydrate interaction, similar to the situation mentioned above for whole body lipid biosynthetic rate. Finally, as also was the case for whole-body lipid biosynthesis, there was a significant protein × carbohydrate coefficient for the SW morph (−4.88 ± 1.99, P < 0.05), but not for the LW(f) morph (1.71 ± 3.09, ns; Table 3). This was due to the increased amount of biosynthesized somatic lipid produced in SW, but not LW(f) morphs, fed on diets at the edges of the response surface (Fig. 2A, B).

3.4. Ovarian lipid allocation

In contrast to the situation for whole-body or somatic lipid, amount of newly biosynthesized lipid found in the ovaries was higher in SW (1.63 ± 0.12%, N = 53) compared with LW(f) females (0.92 ± 0.13%; N = 56) across the protein-carbohydrate landscape (Fig 2B, C; Partial F-test of full and reduced models: $F_{6,97}$ = 3.47, P = 0.0014; Table 1; Appendix 3D). Biosynthesized lipid in the ovaries was uniform across the protein-carbohydrate landscape in the LW(f) morph (Fig 2C; no significant linear or quadratic response surface terms for protein, carbohydrate or interactions; Table 3). In the SW morph, a greater amount of biosynthesized lipid in the ovaries was associated with increasing protein content of the diet (Fig 2D; linear coefficient for protein: 0.56 ± 0.25, P < 0.05, Table 3). Rates also increased with increasing carbohydrate content of the diet, although the linear carbohydrate coefficient was non-significant (0.40 ± 0.25, ns) and there was a significant protein × carbohydrate interaction in the SW morph (Fig 2D; protein × carbohydrate coefficient: −0.96 + 0.45, P < 0.05, Table 3). When ovarian mass was used as a covariate in an ANCOVA, no significant effect of morph or diet was observed on the amount of biosynthesized lipid in the ovary (partial F-test of full and reduced models: $F_{6,96}$ = 0.47, ns). This indicates that the greater amount of biosynthesized lipid in the ovaries of SW females appears to be associated entirely with the larger size of the ovaries in that morph.

Table 3
Coefficients (β ± s.e.m.) indicating the magnitude and significance of linear and quadratic aspects of response surfaces of somatic lipid allocation, ovarian lipid allocation, and proportional allocation to the soma for response surfaces of LW(f) and SW morphs presented in Fig. 2.

Model terms	Somatic lipid allocation		Ovarian lipid allocation		Proportional allocation to soma	
Morph	LW(f)	SW	LW(f)	SW	LW(f)	SW
Intercept	9.30 ± 6.74	4.71 ± 5.25	**0.98 ± 0.16**	**1.31 ± 0.30**	**0.936 ± 0.013**	**0.851 ± 0.024**
Initial cricket mass (covariate)	0.01 ± 0.01	0.003 ± 0.006				
Protein	2.48 ± 1.49	0.42 ± 1.06	0.21 ± 0.14	**0.56 ± 0.25**	−0.002 ± 0.011	*−0.039 ± 0.021*
Carbohydrate	**8.34 ± 1.65**	**2.26 ± 1.04**	0.28 ± 0.15	0.40 ± 0.25	**0.028 ± 0.012**	0.000 ± 0.021
Protein × Protein	3.53 ± 2.43	2.30 ± 1.79	−0.05 ± 0.25	0.16 ± 0.44	0.020 ± 0.019	0.012 ± 0.037
Carbohydrate × Carbohydrate	−3.39 ± 2.81	*3.72 ± 1.97*	−0.06 ± 0.27	*0.73 ± 0.46*	*−0.041 ± 0.021*	−0.039 ± 0.038
Protein × Carbohydrate	1.71 ± 3.09	**−4.88 ± 1.99**	−0.51 ± 0.28	**−0.96 ± 0.45**	0.020 ± 0.021	0.015 ± 0.037
R^2 (adjusted)	0.31	0.15	0.09	0.10	0.10	−0.01
Model significance	**$F_{6,61}$ = 6.11, *P* < 0.001**	**$F_{6,40}$ = 15.5, *P* < 0.001**	$F_{5,47}$ = 2.04, P = 0.09	**F5,50 = 3.04, P = 0.02**	*$F_{5,47}$ = 2.13, P = 0.08*	**$F_{5,50}$ = 2.49, *P* = 0.04**

Coefficients were estimated using general linear models. Protein and carbohydrate model terms were standardized to a scale from −1 to 1. Terms in bold are significant at the α < 0.05 level, and italicized terms are borderline significant (α < 0.10). Negative quadratic regression coefficients indicate a peak (convex) relationship, whereas positive quadratic regression coefficients indicate a trough (concave) relationship. The most inclusive models are presented to facilitate comparisons between the morphs. See Materials and Methods for explanation of "linear" and "quadratic" coefficients.

3.5. Morph-specific trade-off of allocation of biosynthesized lipid to somatic vs ovarian body compartments

Over the entire protein-carbohydrate landscape, the percentage of whole-body radiolabeled lipid found in the somatic versus ovarian compartments was significantly higher in the LW(f) morph (93.0 ± 1.01%; N = 53) compared with the SW morph (84.0 ± 0.96%; N = 56; Partial F-test: $F_{6,97} = 7.71$, $P < 0.001$; Fig 2E, F; Table 1; Appendix 3E). Across morphs, there was no overall effect of either major dietary macronutrient on the degree of newly biosynthesized lipid allocated to the somatic vs. ovarian body compartments ($P > 0.1$ for either protein or carbohydrate, Table 3; Appendix 3E). However, within the LW(f) morph there was a significant linear coefficient for carbohydrate (0.028 ± 0.012, $P < 0.05$; Table 3) compared to a non-significant coefficient in the SW morph (Table 3). Inspection of the response surfaces (Fig 2E, F) indicates that this was due to a significantly greater allocation of biosynthesized lipid to the soma with increasing carbohydrate in the diet.

3.6. $NADP^+$-IDH specific activity

Like the rate of whole-body or somatic lipid biosynthesis, $NADP^+$-IDH specific activity of the fat body was significantly higher in the LW(f) morph compared to the SW morph across the entire protein-carbohydrate landscape (morph means (±SEM): LW(f) = 233.1 ± 11.2, SW = 169.2 ± 7.1 nmol/min/mg protein; Fig 3A, B; Partial F-test: $F_{6,112} = 6.35$, $P < 0.001$; Table 1; Appendix 3F). For the LW(f) morph, $NADP^+$-IDH specific activity was essentially uniform across the response surface (Fig 3A), with no significant linear or quadratic terms for protein or carbohydrate (Table 4). By contrast, for the SW morph, $NADP^+$-IDH specific activity rose linearly with carbohydrate content (Fig 3B; carbohydrate linear coefficient = 0.39 ± 0.14, $P < 0.05$, Table 4) and there was a significant quadratic coefficient for carbohydrate (0.74 ± 0.26, $P < 0.05$).

3.7. ACL specific activity

ACL also exhibited a significantly higher fat body specific activity in the LW(f) morph compared to the SW morph (Partial F-test: $F_{6,138} = 6.35$, $P < 0.001$; Table 1; Appendix 3G) across the entire protein-carbohydrate landscape (morph means(±SEM): LW(f) 33.8 ± 2.5, SW = 23.8 ± 2.1Fig 3C, D). However, no significant main effect of morph was observed ($F_{1,138} = 0.23$, $P = 0.63$; Table 1; Fig 3C, D). Neither did protein nor carbohydrate exhibit significant main effects on ACL specific activity ($P > 0.3$, Table 1; Appendix 3G). However, there were numerous (5) significant interaction terms involving various combinations of morph, protein, or carbohydrate (Table 1; Appendix 3G), for example, morph × protein [$F_{1,138} = 10.4$, $P = 0.002$] and morph × carbohydrate × protein ($F_{1,138} = 10.3$, $P = 0.002$). This indicates complex morph-specific response surfaces in which multiple peaks differed in location and height in a morph-specific manner (see Fig. 3C, D). For example, the LW(f) morph exhibited higher peaks of ACL specific activity in the two quadrants of the response surface comprising (1) high-protein, low carbohydrate (e.g. diet p28:c14) and (2) high carbohydrate, low protein (p8:c34). These were not seen in the SW landscape. By contrast, the ACL specific activity response surface of the SW morph exhibited peaks in the other two quadrants (e.g. p9:c12 and p16.25:c35.25) that were not seen in the LW landscape. These qualitative differences were manifest quantitatively as significant coefficients for protein × protein (3.27 ± 1.23, $P < 0.05$) and protein × carbohydrate (−4.73 ± 1.24, $P < 0.05$) in the LW(f) but not SW surfaces (Table 4). Finally, a morph-specific effect of protein on ACL specific activity is evidenced by the significant linear protein coefficient in the SW morph (−1.43 ± 0.59 $P < 0.05$; Table 4) that was not significant in the LW(f) morph.

4. Discussion

The wing-polymorphic cricket, *Gryllus firmus*, has emerged as an important model species in studies of the biochemical basis of life history variation and trade-offs in outbred populations (e.g., Zhao and Zera, 2002; Zera, 2005; Zera and Zhao, 2003, 2006; Zera and Harshman, 2011; Schilder et al., 2011). Although previous investigations documented large magnitude differences between morphs in many aspects of lipid metabolism (see Introduction), the generality of these results was unclear because experiments were mainly conducted on a single artificial diet that contained 20% protein and 27% carbohydrate. In particular, prior experiments could not assess the extent to which the morph-differences in lipid metabolism are dependent upon diet protein-carbohydrate content. In the current study we examined how diet influenced morph-differences in lipid metabolism by conducting radiotracer and enzymological investigations across 13 ecologically relevant diets that differed in their protein-carbohydrate content. Our results confirm and extend key findings of previous biochemical studies, but require reevaluation of others.

4.1. Morph differences in lipid biosynthesis across the protein-carbohydrate landscape

One important finding of the present study was the overall greater rate of whole-body lipid biosynthesis in the LW(f) compared to the SW morph across the entire protein-carbohydrate

Table 4
Coefficients (β ± s.e.m.) indicating the magnitude and significance of linear and quadratic aspects of response surfaces of $NADP^+$-IDH and ACL specific activities of LW(f) and short-winged (SW) morphs presented in Fig 3.

Model terms	$NADP^+$-IDH specific activity		ACL specific activity	
Morph	LW(f)	SW	LW(f)	SW
Intercept	**204 ± 18**	**156 ± 12**	**27.1 ± 4.6**	**24.2 ± 3.9**
Initial cricket mass (covariate)				
Protein	14 ± 14	*-20 ± 12*	3.8 ± 4.1	**−8.6 ± 3.5**
Carbohydrate	16 ± 16	**31 ± 11**	2.4 ± 3.8	**7.6 ± 3.2**
Protein × Protein	23 ± 26	−26 ± 21	**19.6 ± 7.4**	*−11.7 ± 6.3*
Carbohydrate × Carbohydrate	45 ± 31	**59 ± 21**	5.2 ± 7.2	6.4 ± 5.9
Protein × Carbohydrate	−45 ± 28	−7 ± 22	**−28.4 ± 7.4**	2.9 ± 6.3
R^2 (adjusted)	0.05	0.23	0.17	0.16
Model significance	$F_{5,50} = 1.55$, $P = 0.19$	**$F_{5,62} = 4.91$, $P = 0.001$**	**$F_{5,69} = 4.1$, $P = 0.003$**	**$F_{5,69} = 3.86$, $P = 0.004$**

Coefficients were estimated using general linear models. Protein and carbohydrate model terms were standardized to a scale from −1 to 1. Terms in bold are significant at the $\alpha < 0.05$ level, and italicized terms are borderline significant ($\alpha < 0.10$). Negative quadratic regression coefficients indicate a peak (convex) relationship, whereas positive quadratic regression coefficients indicate a trough (concave) relationship. The most inclusive models are presented to facilitate comparisons between the morphs. See Materials and Methods for explanation of "linear" and "quadratic" coefficients.

landscape (Fig. 1C, D). The only local exception to this general pattern was the nearly equal and low biosynthetic rates of the morphs on very low carbohydrate and protein diets (bottom of Fig 1C, D). Thus, the greater rate of lipid biosynthesis of LW(f) vs. SW *G. firmus* reported previously on a limited number of diets (Zhao and Zera, 2002; Zera, 2005), appears to be a general feature of the polymorphism across a wide range of diets. Although crickets are omnivorous, little is known about the exact composition of cricket diets in the field. However, diets used in the present study cover the range of protein and carbohydrate levels found in plants (high carbohydrate, low protein – diets a, b, d and g; see Appendix 1 and Fig. 1A) and animals (lower carbohydrate, higher protein – diets c, i and j). Thus, findings of biochemical and physiological studies of morph-specific lipogenesis conducted in the laboratory on these diets can likely be extrapolated to field environments.

De novo fatty acid and glyceride biosynthesis primarily occur in the fat body, after which newly biosynthesized lipid is either stored in this organ, mainly in the form of triglyceride, or is transported to other organs (e.g. as a component of vitellogenin, transported to the ovaries; Candy, 1985; Ziegler, 1997; Hagedorn and Kunkel, 1979; Klowden, 2002). Because we separately quantified the amount of newly biosynthesized lipid in the soma (body minus ovaries) or ovaries, we could determine the amount that was allocated to each of these body compartments across the protein-carbohydrate landscape. This is important because a central issue in life history physiology concerns the relative allocation of nutrients to somatic vs. reproductive functions (Zera and Harshman, 2001; Harshman and Zera, 2007; Flatt and Heyland, 2011). Lipid is an important energy-rich component of eggs (ca. 25% dry weight of *G. firmus* eggs; Zera et al., 1994) as well as being an important somatic energy reserve. While a number of studies have quantified whole-body lipid in a life history context, the reproductive versus somatic components have not always been separated (Zera and Harshman, 2001). This, in turn, has resulted in overestimates of nutrient allocation to the soma and underestimates in allocation to reproduction, in cases in which whole body lipid has been equated with energetic investment to somatic functions (Zera and Harshman, 2001; Zhao and Zera, 2002; Zera and Harshman, 2011).

In both morphs, the majority of total biosynthesized lipid was found in the soma (85–95%; Fig 2E, F; see below), and the amount of somatic lipid was significantly greater for the LW(f) compared to the SW morph (Fig. 2E, F). This difference was due not only to the greater rate of whole-body lipid biosynthesis (Fig 1C, D), but also to the greater proportion of whole-body lipid biosynthesis allocated to the soma versus ovaries in LW(f) females (93.1 ± 0.7%) vs. SW females (SW: 84.0 ± 1.2%; Fig. 2E, F). In other words, there was a trade-off between the morphs in the extent to which newly biosynthesized lipid was preferentially allocated to the soma versus ovaries over the entire protein-carbohydrate landscape, similar to the morph-specific trade-off observed previously on the standard laboratory diet (Zhao and Zera, 2002). Both elevated lipid biosynthesis and greater allocation to the soma by LW(f) females are likely important contributors to the elevated total somatic lipid content in LW(f) compared to SW females across the entire protein-carbohydrate landscape (Clark et al., 2015; Zera, Clark and Behmer, unpublished data). This current finding suggests that overall morph-specific differences in lipid levels, as reported in Clark et al. (2015), can largely be explained by morph-specific differences in lipid biosynthesis, and not just differences in the amount of carbohydrate eaten. However, the importance of morph-specific differences in lipid oxidation have yet to be taken into account.

In several cases, diet appeared to significantly affect the magnitude of the morph difference in biosynthesized somatic lipid (see Results). Most important was the greater positive effect of carbohydrate on lipid production in LW(f) compared with SW *G. firmus* (Fig 1C, D). This was associated with a greater relative increase of whole-body lipogenesis in LW(f) compared to SW in the high carbohydrate region of the protein-carbohydrate landscape. In addition, the relative amount of lipid allocated to the soma versus the ovaries (i.e. the magnitude of the somatic-ovarian trade-off) was also greater in LW(f) vs SW females on high carbohydrate diets (Fig 2E, F). The positive effect of dietary carbohydrate on lipid biosynthesis in animals has been well-known for decades (MacDonald, 1966; Hori and Nakasone, 1971; Geer and Perille, 1977; Groener and van Golde, 1977; Goodridge, 1987; Girard et al., 1997), as has the influence of genotype of laboratory stocks on the degree to which lipogenesis is affected by dietary carbohydrate (Berdanier et al., 1979; Geer and Laurie-Ahlberg, 1984; Reed et al., 2010; Musselman et al., 2013). A unique aspect of the present study is the demonstration that diet protein-carbohydrate profile appears to strongly influence the magnitude of lipid biosynthesis differences between morphs of *G. firmus*. Across the landscape, this could be due to several factors that may act in concert. The LW(f) morph might be inherently programmed to divert more carbohydrate to lipid on high carbohydrate diets even when an equal amount of carbohydrate is consumed by the morphs (i.e. pathway enzymes in the LW(f) morph might be more sensitive to carbohydrate or carbohydrate derivatives). Alternatively, greater consumption by the LW(f) morph on high carbohydrate diets might provide more substrate for lipogenesis. A previous feeding study demonstrated greater food consumption for the LW(f) morph compared with the SW morph on some but not all diets in the high carbohydrate region of the nutrient landscape (see Fig. 2C of Clark et al. (2015)).

The much smaller effect of carbohydrate on lipid allocation to the soma in the SW morph might be due to a constraint in the degree to which lipid can be stored in the soma relative to the LW(f) morph. On the standard laboratory diet, SW females, compared to LW(f) females, have about half the amount of fat body (Zera and Zhao, 2003; and unpublished data), possibly due to the much larger ovaries in the SW morph coupled with limited thoracic and abdominal space. Increased ovarian mass in SW females likely occurs at the expense of fat body mass, thus limiting somatic lipid storage capacity. Recent studies indicate that the ability to convert carbohydrate into lipid is not only important with respect to producing somatic and reproductive energy reserves, it also serves as a mechanism by which organisms (including insects such as *Drosophila*) tolerate high carbohydrate diets by converting carbohydrate into lipid, because it reduces glucose concentration in the blood (Musselman et al., 2013). An emerging concept in human diabetes research is that fat accumulation per se is less harmful than the production of free fatty acids and their derivatives, which occurs when the capacity of the organism to convert fatty acids to triglyceride stores in the fat body is exceeded (termed "lipotoxicity"; Brookheart et al., 2009; Neuschwander-Tetri, 2010). This suggests that, if the SW morph of *G. firmus* has reduced ability to convert dietary carbohydrate into stored triglyceride, this morph might be more sensitive to the deleterious effect of a high carbohydrate diet than the LW(f) morph. Consistent with this hypothesis, preliminary data indicate that glucose oxidation is higher in SW than in LW(f) females across the protein-carbohydrate landscape in these LW(f) and SW populations (Zera, Clark, Behmer, unpubl data). In addition a greater proportion of carbohydrates is oxidized on high carbohydrate diets by both morphs (Clark et al., 2016).

SW females allocated a greater amount of biosythesized lipid than LW(f) females to the ovaries over the entire protein-carbohydrate landscape (Fig 2C, D); this was expected because SW females have larger ovaries. However, the morph-specific pattern of lipid allocation to the ovaries differed from that in the soma in some respects. Ovarian allocation was relatively low and uniform across the protein-carbohydrate landscape in LW(f) females

(Fig 2C). By contrast, SW females increased lipid allocation to the ovaries as a function of dietary protein, and to a lesser degree (and non-significantly) as a function of dietary carbohydrate. Ovarian mass was substantially higher in SW versus LW(f) females across the entire protein-carbohydrate landscape, but especially so in the high protein region (Fig 2D). Thus, the greater allocation of lipid to the ovaries on high protein diets in SW females might be a requirement to accommodate greater growth of eggs on those diets, because eggs have a high lipid content (ca. 25% dry mass; Zera et al., 1994).

4.2. Morph-specific differences in enzyme activities across the protein-carbohydrate landscape

In previous studies on the standard laboratory diet, a straightforward relationship was observed between specific activities of five lipogenic enzymes, including fat body NADP$^+$-IDH and ACL, and rate of lipid biosynthesis. Specific activities of all lipogenic enzymes as well as the rate of lipid biosynthesis were elevated to a similar degree in the LW(f) compared to the SW morph, and strongly co-segregated with the LW(f) morph in crosses between the LW(f) and SW stocks (Zera and Zhao, 2003). This result suggested that morphs might differ genetically in a few regulators that co-ordinate many aspects of lipid metabolism (Zera and Zhao, 2003). In the present study, undertaken across a wider range of diets, less concordant patterns were observed between specific activities of lipogenic enzymes and rate of lipid biosynthesis.

As in previous studies, specific activities for NADP$^+$-IDH were higher in LW(f) than SW females across the entire protein-carbohydrate landscape (Fig 3A, B). This is consistent with elevated NADP$^+$-IDH activity contributing in a general way to higher rates of lipid biosynthesis in LW(f) females across all diets (Fig 1C, D). Nevertheless, on the highest carbohydrate diets, activities of this enzyme were similar in LW(f) and SW crickets, due to the positive effect of dietary carbohydrate on NADP$^+$-IDH activity in SW, but not LW(f) females (Fig. 3A, B). These patterns did not match the much greater rate of lipid biosynthesis in the LW(f) morph on the high carbohydrate diets, nor the positive effect of carbohydrate on lipid biosynthesis in LW(f) but not SW females (see above).

One possible explanation for this discordant pattern is that NADP$^+$-IDH might be a less important contributor to morph-specific differences in lipid biosynthesis in the high –carbohydrate region of the nutrient landscape. A variety of enzymes other than NADP$^+$-IDH contribute NADPH for lipid biosynthesis (e.g. malic enzyme (ME), glucose-6-phosphate dehydrogenase (G-6-PDH), and 6-phosphogluconate dehydrogenase(6-PGDH)). In *D. melanogaster*, the pentose-shunt enzymes, G-6-PDH and G-PGDH appear to be more important than NADP$^+$-IDH in lipogensis on high-carbohydrate diets (Geer et al., 1978). More recently, Rzezniczak and Merritt (2012) reported complex interactions among NADPH-producing enzymes in *D. melanogaster* in different environments. This further suggests that individual NADP$^+$-producing enzymes, such as NADP$^+$-IDH in *G. firmus,* may have unexpected environment-contingent roles in metabolism.

ATP-citrate lyase (ACL), the other lipogenic enzyme investigated, showed particularly complex patterns of fat-body specific activities in which morph-specific differences in activity of this enzyme were strongly contingent upon diet (Fig. 3C, D). On the one hand, the significantly higher ACL specific activity in LW(f) vs. SW females fed high protein-low carbohydrate diets suggests that this enzyme might be especially important in contributing to the greater lipid biosynthesis in LW(f) compared to SW females on this part of the nutrient landscape. Surprisingly, like NADP$^+$-IDH, ACL specific activity was also not correlated with the highest rates of lipid biosynthesis in the LW(f) morph, which occurred on the highest carbohydrate diets. Results of studies on NADP$^+$-IDH and ACL specific activities to date suggest a complex shifting of importance of various enzymes in contributing to morph-specific differences in lipid biosynthesis across the nutrient landscape. This picture contrasts with the more simplified picture previously proposed regarding the role of variation in lipogenic enzyme activities and lipid biosynthesis (Zera and Zhao, 2003; see above), and is more consistent with the view of strong environment-dependent interactions of enzyme networks (Rzezniczak and Merritt, 2012).

Another intriguing possibility is that variation in activities of lipogenic enzymes other than those involved in fatty acid biosynthesis might be more important with respect to causing morph-specific differences in lipogenesis across the nutrient landscape. Most newly biosythesized lipid in *G. firmus* is triglyceride (85%; Zhao and Zera, 2002; and unpublished), which is produced by enzymes of the glyceride pathway which link fatty acids to the glycerol-3-phosphate backbone. The glyceride pathway functions downstream of the pathway of *de novo* fatty acid biosynthesis in which acetyl-CoA is converted to fatty acid. Thus far, all enzymes whose activities have been measured in morphs of *G. firmus* in the context of lipid biosynthesis (e.g. ACL and NADP$^+$-IDH in the present study) are involved in fatty acid biosynthesis. However, a recent transcriptome study identified morph differences in gene expression of some enzymes of glyceride biosynthesis, as well as enzymes involved in modification of fatty acids such as elongases, reductases, and desaturases, as being much larger than those of genes encoding enzymes of *de novo* fatty acid biosynthesis (Vellichirammal et al., 2014). This suggests that enzymes involved in lipogenesis, that are downstream from *de novo* fatty acid biosynthesis, may play a more important role in regulating morph differences in overall triglyceride production.

Finally, both NADP$^+$-IDH and ACL are involved in metabolic roles other than lipogenesis. For example, in many organisms undergoing oxidative stress, NADP$^+$-IDH produces NADPH, which is subsequently used to produce antioxidants such as reduced glutathione (Lee et al., 2002; Rzezniczak and Merritt, 2012; Dey et al., 2016). Thus, it is conceivable that the unexpected greater increase in NADP$^+$-IDH in the SW morph on high carbohydrate diets, mentioned above, may combat increased oxidative stress, which often accompanies lipotoxicity (Brookheart et al., 2009). In the same vein, high ACL activity occurs in some organs for purposes other than increased lipogenesis, for example, to metabolize citrate as part of the mechanism of hormonal secretion (Guay et al., 2007). There are many possible reasons for the unexpected morph- and diet-specific patterns of NADP$^+$-IDH and ACL activities. These results highlight our ignorance of the specific roles played by enzymes in morph specific-metabolic adaptation to nutrient heterogeneity.

Funding

This work was supported by the National Science Foundation [Grant No. IOS-1121960 to S.T.B. and IOS-1122075 to A.J.Z.].

Appendix 1
Protein and carbohydrate contents of diets used in the present experiment.

Diet protein:carbohydrate content		Total macronutrients (% dry mass)
(a) p4:c17	very carbohydrate biased[1]	21
(b) p9:c12	balanced	" "
(c) p14:c7	very protein-biased	" "
(d) p9.75:c21.75	carbohydrate-biased	31.5
(e) p17.25:c14.25	protein-biased	" "
(f) p8:c34	very carbohydrate-biased	42
(g) p13:c29	carbohydrate-biased	" "
(h) p18:c24	balanced	" "
(i) p23:c19	protein-biased	" "
(j) p28:c14	very protein-biased	" "
(k) p16.25:c36.25	carbohydrate-biased	52.5
(l) p28.75:c23.75	protein-biased	
(m) p27:c36	balanced	63
Total		

[1]Diet treatments are centered around a protein-to-carbohydrate (p:c) ratio of three parts protein to four parts carbohydrate (~p3:c4; "balanced" ratio). This is the average ratio that crickets self-select when they are allowed to choose between a high-protein diet and high-carbohydrate diet (see Clark et al. (2013)).

Appendix 2

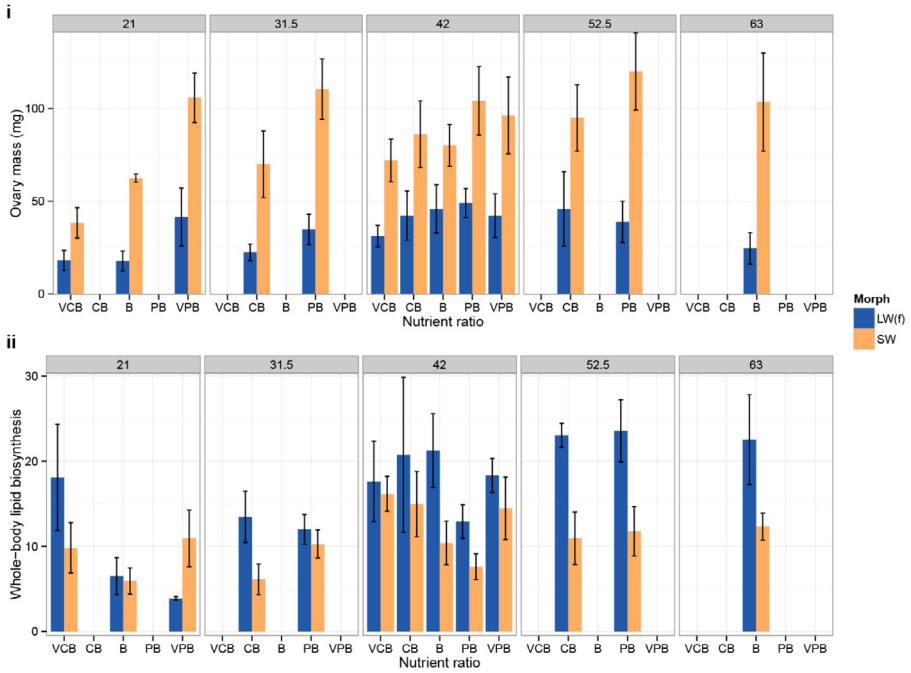

Appendix 2A. Mean ovary masses (i) and rates of whole-body lipid biosynthesis (ii) ±s.e.m. in long-winged [LW(f)] and short-winged (SW) *Gryllus firmus* females reared on one of 13 diets with different amounts and ratios of protein-to carbohydrate. Numbers in the gray boxes at the top of each subpanel indicate the total macronutrient concentration as a percentage of diet dry weight, ranging from 21% to 63%, as further described in Appendix 1. Letters along the x-axis indicate the five nutrient ratios used: very carbohydrate-biased (VCB), carbohydrate-biased (CB), balanced (B), protein-biased (PB), and very protein-biased (VPB). Corresponds with Fig. 1 in the main text.

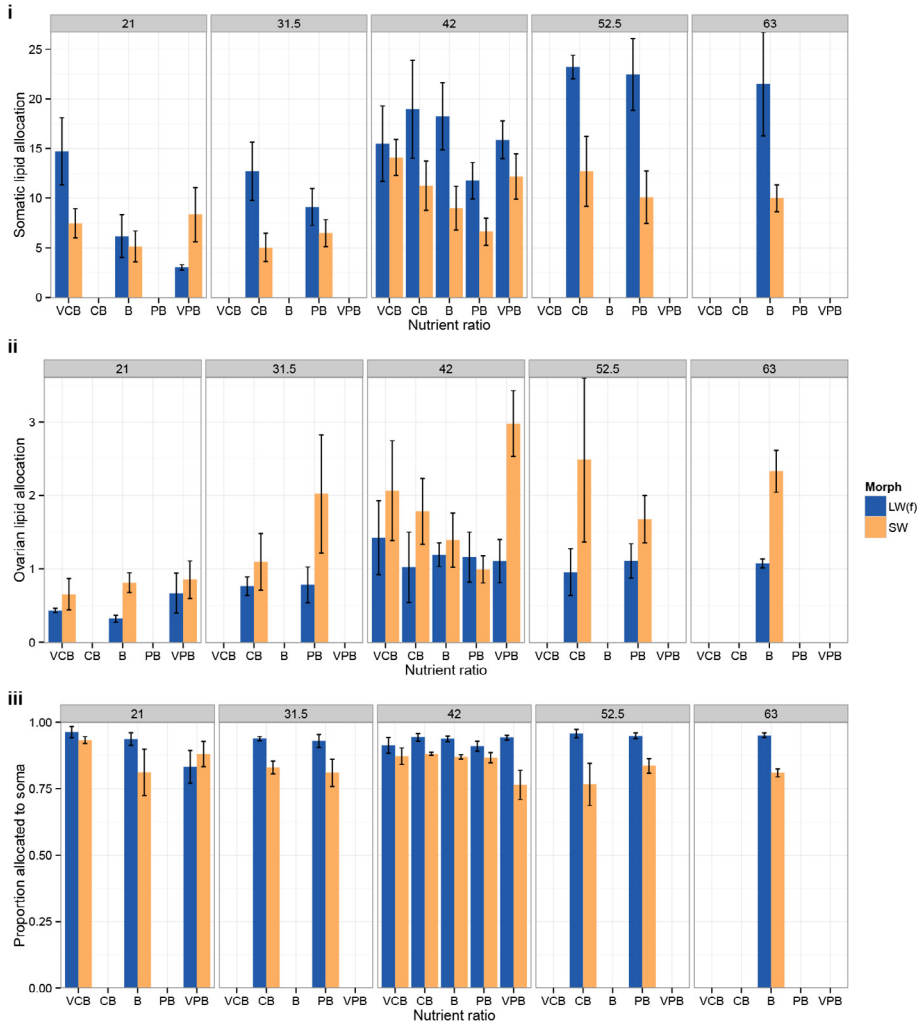

Appendix 2b. Diet means ± s.e.m. for somatic lipid allocation (i), ovarian lipid allocation (ii), and the proportion of lipids allocated to the soma (iii), for long-winged [LW(f)] and short-winged (SW) *G. firmus* females. See Appendix 2A for detailed descriptions of subpanel titles and x-axis labels. Corresponds with Fig. 2 in the main text.

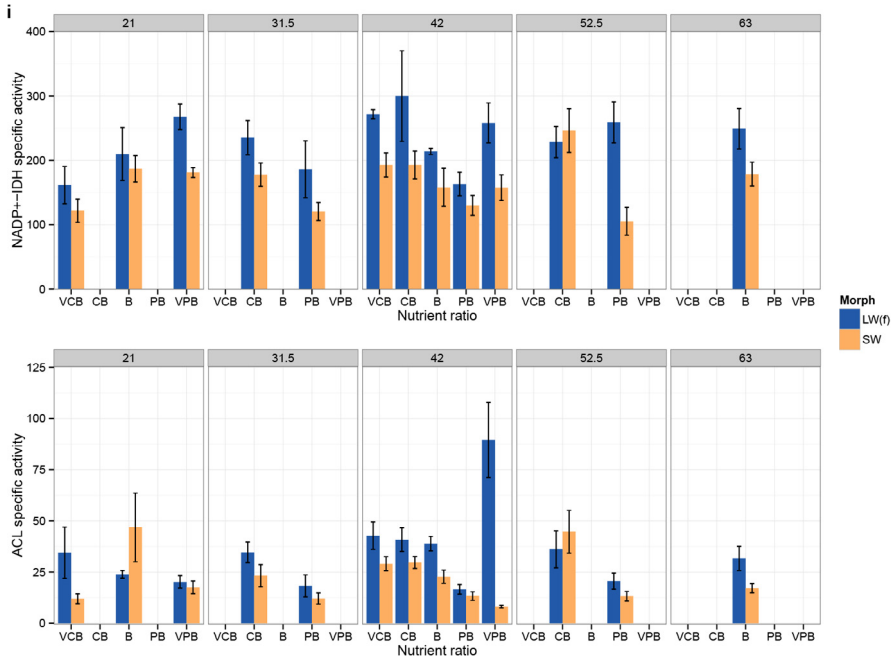

Appendix 2C. Diet means ± s.e.m. for NADP$^+$-IDH (i) and ACL (ii) enzyme specific activity for long-winged [LW(f)] and short-winged (SW) *G. firmus* females. See Appendix 2A for detailed descriptions of subpanel titles and x-axis labels. Corresponds with Fig. 3 in the main text.

Appendix 3

Full ANCOVA/ANOVA tables of effects of morph and dietary components on various response variables. Table 1 in the main text contains a summary of these analyses.

Appendix 3A. Corresponds with Fig. 1A and B.
Measure: Ovary mass

Source	Type III SS	df	MS	F	P	
Full Model	169986	12	14166	19.29	**<0.001**	***
Intercept	18500	1	18500	25.19	**<0.001**	***
Cricket mass (covariate)	42278	1	42278	57.57	**<0.001**	***
Morph	18299	1	18299	24.92	**<0.001**	***
Protein	259	1	259	0.35	0.553	
Carbohydrate	1044	1	1044	1.42	0.235	
Protein × Protein	427	1	427	0.58	0.447	
Carbohydrate × Carbohydrate	2	1	2	0.00	0.959	
Protein × Carbohydrate	1094	1	1094	1.49	0.224	
Morph × Protein	5003	1	5003	6.81	**0.010**	**
Morph × Carbohydrate	2	1	2	0.00	0.962	
Morph × Protein^2	343	1	343	0.47	0.495	
Morph × Carbohydrate^2	86	1	86	0.12	0.733	
Morph × Protein × Carbohydrate	1263	1	1263	1.72	0.192	
Error	92528	126	734			
Adjusted R-squared = 0.6139						
Partial F-test against model without "Morph"		6, 126		15.44	**<0.001**	***

Appendix 3B. Corresponds with Fig. 1C and D.
Measure: Total lipid biosynthesis (whole-body)

Source	Type III SS	df	MS	F	P	
Full Model	2603.23	12	216.94	5.11	**<0.001**	***
Intercept	117.30	1	117.30	2.76	*0.100*	.
Cricket mass (covariate)	84.10	1	84.10	1.98	0.160	
Morph	387.40	1	387.40	9.12	**0.003**	**
Protein	74.50	1	74.50	1.75	0.188	
Carbohydrate	873.10	1	873.10	20.56	**<0.001**	***
Protein × Protein	99.00	1	99.00	2.33	0.130	
Carbohydrate × Carbohydrate	68.50	1	68.50	1.61	0.207	
Protein × Carbohydrate	0.20	1	0.20	0.01	0.940	
Morph × Protein	33.30	1	33.30	0.78	0.378	
Morph × Carbohydrate	307.30	1	307.30	7.24	**0.008**	**
Morph × Protein^2	7.90	1	7.90	0.19	0.667	
Morph × Carbohydrate^2	118.50	1	118.50	2.79	*0.098*	.
Morph × Protein × Carbohydrate	58.50	1	58.50	1.38	0.242	
Error	4076.30	96	42.46			
Adjusted R-squared = 0.3135						
Partial F-test against model without "Morph"		6, 96		5.74	**0.000**	***

Appendix 3C. Corresponds with Fig. 2A and B.
Measure: Somatic lipid allocation

Source	Type III SS	df	MS	F	P	
Full Model	3410.82	12	284.23	7.54	**<0.001**	***
Intercept	238.90	1	238.90	6.34	**0.013**	*
Cricket mass (covariate)	38.10	1	38.10	1.01	0.129	
Morph	539.60	1	539.60	14.32	**0.000**	***
Protein	151.40	1	151.40	4.02	**0.047**	*
Carbohydrate	1340.30	1	1340.30	35.56	**<0.001**	***
Protein × Protein	100.70	1	100.70	2.67	0.105	
Carbohydrate × Carbohydrate	72.70	1	72.70	1.93	0.167	
Protein × Carbohydrate	16.30	1	16.30	0.43	0.512	
Morph × Protein	62.00	1	62.00	1.64	0.202	
Morph × Carbohydrate	419.30	1	419.30	11.13	**0.001**	**
Morph × Protein^2	5.00	1	5.00	0.13	0.715	
Morph × Carbohydrate^2	161.40	1	161.40	4.28	**0.041**	*
Morph × Protein × Carbohydrate	124.30	1	124.30	3.30	*0.072*	.
Error	4673.80	124	37.69			
Adjusted R-squared = 0.3659						
Partial F-test against model without "Morph"		6, 124		8.23	<0.001	***

Appendix 3D. Corresponds with Fig. 2C and D.
Measure: Ovary lipid allocation

Source	Type III SS	df	MS	F	P	
Full Model	37.85	12	3.15	4.04	**<0.001**	***
Intercept	12.88	1	12.88	16.49	**<0.001**	***
Morph	0.73	1	0.73	0.94	0.335	
Protein	0.78	1	0.78	0.99	0.322	
Carbohydrate	1.14	1	1.14	1.46	0.229	
Protein × Protein	0.01	1	0.01	0.02	0.900	
Carbohydrate × Carbohydrate	0.02	1	0.02	0.02	0.890	

Appendix 3 (*continued*)

Appendix 3D. Corresponds with Fig. 2C and D.
Measure: Ovary lipid allocation

Source	Type III SS	df	MS	F	P	
Protein × Carbohydrate	1.18	1	1.18	1.52	0.221	
Morph × Protein	1.13	1	1.13	1.44	0.233	
Morph × Carbohydrate	0.14	1	0.14	0.17	0.677	
Morph × Protein^2	0.12	1	0.12	0.16	0.691	
Morph × Carbohydrate^2	1.64	1	1.64	2.10	0.151	
Morph × Protein × Carbohydrate	0.49	1	0.49	0.63	0.429	
Error	75.75	97	0.78			
Adjusted R-squared = 0.2364						
Partial F-test against model without "Morph"		6, 97		3.47	**0.004**	**

Appendix 3E. Corresponds with Fig. 2E and F.
Measure: Proportion of lipid allocated to soma (vs. ovaries)

Source	Type III SS	df	MS	F	P	
Full Model	0.2803	11	0.0255	4.91	**<0.001**	***
Intercept	11.7803	1	11.7803	2,267.15	**<0.001**	***
Morph	0.0489	1	0.0489	9.41	**0.003**	**
Protein	0.0000	1	0.0000	0.01	0.926	
Carbohydrate	0.0122	1	0.0122	2.35	0.128	
Protein × Protein	0.0022	1	0.0022	0.43	0.513	
Carbohydrate × Carbohydrate	0.0081	1	0.0081	1.56	0.215	
Protein × Carbohydrate	0.0030	1	0.0030	0.38	0.540	
Morph × Protein	0.0133	1	0.0133	2.56	0.113	
Morph × Carbohydrate	0.0066	1	0.0066	1.28	0.262	
Morph × Protein^2	0.0002	1	0.0002	0.03	0.856	
Morph × Carbohydrate^2	0.0000	1	0.0000	0.00	0.969	
Morph × Protein × Carbohydrate	0.0001	1	0.0001	0.02	0.892	
Error	0.5040	97	0.0052			
Adjusted R-squared = 0.2846						
Partial F-test against model without "Morph"		6, 97		7.71	**<0.001**	***

Appendix 3F. Corresponds with Fig. 3A and B.
Measure: NADP$^+$-IDH Specific Activity

Source	Type III SS	df	MS	F	P	
Full Model (no covariates)	193582	11	17598	5.49	**<0.001**	***
Intercept	514379	1	514379	160.38	**<0.001**	***
Morph	16406	1	16406	5.12	**0.026**	*
Protein	3851	1	3851	1.20	0.276	
Carbohydrate	3874	1	3874	1.21	0.274	
Protein × Protein	2929	1	2929	0.91	0.341	
Carbohydrate × Carbohydrate	7792	1	7792	2.43	0.122	
Protein × Carbohydrate	10145	1	10145	3.16	*0.078*	.
Morph × Protein	11615	1	11615	3.62	*0.060*	.
Morph × Carbohydrate	2279	1	2279	0.71	0.401	
Morph × Protein^2	6835	1	6835	2.13	0.147	
Morph × Carbohydrate^2	499	1	499	0.16	0.694	
Morph × Protein × Carbohydrate	3656	1	3656	1.14	2.880	
Error	359216	112	3207			
Adjusted R-squared = 0.2864						
Partial F-test against model without "Morph"		6, 112		6.35	**<0.001**	

Appendix 3G. Corresponds with Fig. 3C and D.
Measure: ACL-Specific Activity

Source	Type III SS	df	MS	F	P	
Full Model (no covariates)	17430	11	1585	4.59	**<0.001**	***
Intercept	13684	1	13684	39.66	**<0.001**	***
Morph	79	1	79	0.23	0.632	
Protein	347	1	347	1.00	0.318	
Carbohydrate	162	1	162	0.47	0.494	
Protein × Protein	2834	1	2834	8.21	**0.005**	**
Carbohydrate × Carbohydrate	207	1	207	0.60	0.439	
Protein × Carbohydrate	5834	1	5834	16.91	**<0.001**	***
Morph × Protein	1785	1	1785	5.17	**0.024**	*
Morph × Carbohydrate	383	1	383	1.11	0.294	
Morph × Protein^2	3588	1	3588	10.40	**0.002**	**
Morph × Carbohydrate^2	6	1	6	0.02	0.897	
Morph × Protein × Carbohydrate	3553	1	3553	10.30	**0.002**	**
Error	47608	138	345			
Adjusted R-squared = 0.2097						
Partial F-test against model without "Morph"		6, 138		6.35	**<0.001**	***

References

Behmer, S.T., 2009. Insect herbivore nutrient regulation. Annu. Rev. Entomol. 54, 165–187.

Berdanier, C.D., Tobin, R.B., Devore, A., 1979. Effect of age, strain, and dietary carbohydrate on the hepatic metabolism of male rats. J. Nutr. 109, 261–271.

Boggs, C.L., 2009. Understanding insect life histories and senescence through a resource allocation lens. Funct. Ecol. 23, 27–37.

Brookheart, R.T., Michel, C.I., Schaffer, J.E., 2009. As a matter of fat. Cell Metab. 10, 9–12.

Candy, D.J., 1985. Intermediary metabolism. In: Kerkut, G.A., Gilbert, L.I. (Eds.), Comprehensive Insect Physiology Biochemistry and Pharmacology. Pergamon, Oxford, pp. 1–41.

Clark, R.M., McConnell, A., Zera, A.J., Behmer, S.T., 2013. Nutrient regulation strategies differ between cricket morphs that trade-off dispersal and reproduction. Funct. Ecol. 27, 1126–1133.

Clark, R.M., Zera, A.J., Behmer, S.T., 2015. Nutritional physiology of life-history trade-offs: how food protein-carbohydrate content influences life-history traits in the wing-polymorphic cricket *Gryllus firmus*. J. Exp. Biol. 218, 1–11.

Clark, R.M., Zera, A.J., Behmer, S.T., 2016. Metabolic rate is canalized in the face of variable life history and nutritional environment. Funct. Ecol. 30, 922–931.

Dey, S., Sidor, A., O'Rourke, B., 2016. Compartment-specific control of reactive oxygen species scavenging by antioxidant pathway enzymes. J. Biol. Chem. 291, 11185–11192.

Flatt, T., Heyland, A., 2011. Mechanisms of Life History Evolution. Oxford University Press, Oxford.

Furrer, R., Nychka, D., Sain, S. 2012. fields: tools for spatial data (Version 6.7). Retrieved from <http://CRAN.R-project.org/package=fields>.

Geer, B.W., Perille, T.J., 1977. Effects of deitary sucrose and environmental temperature on fatty acid synthesis in *Drosophila melanogaster*. Insect Biochem. 7, 371–379.

Geer, B.W., Woodward, C.G., Marshall, S.D., 1978. Regulation of the oxidative NADP-enzyme tissue levels in *Drosophila melanogaster*. II The biochemical basis of dietary carbohydrate and D-glycerate modulation. J. Exp. Zool. 203, 391–402.

Geer, B.W., Laurie-Ahlberg, C.C., 1984. Genetic variation in the dietary sucrose modulation of enzyme activities in *Drosophila melanogaster*. Genet. Res. Cambridge 43, 307–321.

Girard, J., Ferre, P., Foufelle, F., 1997. Mechanisms by which carbohydrates regulate expression of genes for glycolytic and lipogenic enzymes. Annu. Rev. Nutr. 17, 325–352.

Goodridge, A.G., 1987. Dietary regulation of gene expression: enzymes involved in carbohydrate and lipid metabolism. Annu. Rev. Nutr. 7, 157–185.

Groener, J.E.M., van Golde, L.M.G., 1977. Effect of fasting and feeding a high-sucrose, fat-free diet on the synthesis of hepatic glycerolipids *in vivo* and in isolated hepatocytes. Biochem. Biophys. Acta 487, 105–114.

Guay, C., Madiraju, S.R., Aumais, J.E., Prentki, M., 2007. A role for ATP-citrate lyase, malic enzyme and pyruvate/citrate cycling in glucose-induced insulin secretion. J. Biol. Chem. 282, 3565–3567.

Guerra, P.A., 2011. Evaluating the life history trade-off between dispersal capability and reproduction in wing dimorphic insects: a meta-analysis. Biol. Rev. 86, 813–835.

Hagedorn, H.H., Kunkel, J.G., 1979. Vitellogenin and vitellin in insects. Annu. Rev. Entomol. 24, 475–505.

Harrison, R.G., 1980. Dispersal polymorphisms in insects. Annu. Rev. Ecol. Syst. 11, 95–118.

Harshman, L.G., Zera, A.J., 2007. The cost of reproduction: the devil in the details. Trend Ecol. Evol. 22, 80–86.

Hori, Y., Nakasone, S., 1971. Effects of the levels of fatty acids and carbohydrates in a diet on the biosynthesis of fatty acids in the larvae of the silkworm, Bombyx mori. J. Insect Physiol. 17, 1441–1450.

Klowden, M., 2002. Physiological Systems in Insects. Academic Press, Amsterdam.

Lee, S.M., Koh, H.-J., Park, D.-C., Song, B.J., Huh, T.-L., Park, J.-W., 2002. Cytosolic NADP+-dependent isocitrate dehydrogenase status modulates oxidative damage to cells. Free Radical Biol. Med. 32, 1185–1196.

Lee, K.P., Simpson, S.J., Clissold, F.J., Brooks, R., Ballard, J.W.O., Taylor, P.W., Soran, N., Raubenheimer, D., 2008. Lifespan and reproduction in *Drosophila*: New insights from nutritional geometry. Proc. Natl. Acad. Sci. U.S.A. 105, 2498–2503.

Lenth, R.V., 2009. Response-surface methods in R, using rsm. J. Stat. Soft. 32, 1–17.

MacDonald, I., 1966. Lipid responses to dietary carbohydrates. Adv. Lipid Res. 4, 39–67.

Musselman, L.P., Fink, J.L., Vankatesh, P., Patterson, B.W., Okunade, A.L., Maier, E., Brent, M.R., Turk, J., Baranski, T.J., 2013. Role of fat body lipogenesis in protection against the effects of caloric overload in *Drosophila*. J. Biol. Chem. 288, 8028–8042.

Neuschwander-Tetri, B.A., 2010. Nontriglyceride hepatic lipotxicity: the new paradigm for the pathogenesis of NASH. Curr. Gastroenterol. Rep. 12, 49–56.

Reed, L.K., Williams, S., Springston, M., Brown, J., Freeman, DesRoches, K.C.E., Sokolowski, M.B., Gibson, G., 2010. Genotype-by-diet interactions drive metabolic phenotypic variation in Drosophila melanogaster. Genetics 185, 1009–1019.

Rzezniczak, T.Z., Merritt, T.J., 2012. Interactions of NADP-reducing enzymes across varying environmental conditions: a model of biological complexity. Genes, Genomes, Genet. 2, 1613–1623.

Schilder, R.J., Zera, A.J., Black, C., Hoidel, M., Wehrkamp, C., 2011. The biochemical basis of life history adaptation: Molecular/enzymological causes of $NADP^+$-isocitrate dehydrogenase activity differences between morphs of *Gryllus firmus* that differ in lipid biosynthesis and life history. Mol. Biol. Evol. 28, 3381–3393.

Simpson, S.J., Raubenheimer, D., 1999. Assuaging nutritional complexity: a geometrical approach. Proc. Nutr. Sci. 58, 779–789.

Simpson, S.J., Raubenheimer, D., 2012. The Nature of Nutrition. A unifying framework from animal adaptation to human obesity. Princeton University Press, Princeton.

Stoscheck, C.M., 1990. Quantitation of protein. Method Enzymol. 182, 60–63.

van Noordwijk, A.J., de Jong, G., 1986. Acquistion and allocation of resources: their influence on variation in life history tactics. Am. Nat. 128, 137–142.

Vellichirammal, N., Zera, A.J., Schilder, R.J., Wehrkamp, C., Riethoven, J.-J.M., Brisson, J.A., 2014. *De novo* transcriptome assembly from fat body and flight muscle trascripts to identify morph-specific gene expression in *Gryllus firmus*. PLoS One 9, e82129.

Zera, A.J., 2009. Wing polymorphism in *Gryllus* (Orthoptera:Gryllidae): proximate endocrine, energetic and biochemical bases underlying morph specializations for flight vs. reproduction. In: Ananthakrishnan, T., Whitman, D. (Eds.), Phenotypic Plasticity in Insects: Mechanisms and Consequences. Science Publishers, Enfield (NH), pp. 609–653.

Zera, A.J., 2005. Intermediary metabolism and life history trade-offs: lipid metabolism in lines of the wing-polymorphic cricket, *Gryllus firmus*, selected for flight capability vs. early age reproduction. Integr. Comp. Biol. 45, 511–524.

Zera, A.J., Brisson, J.A., 2012. Quantitative, physiological, and molecular genetics of dispersal and migration. In: Colbert, J., Baguette, M., Benton, T., Bullock, J. (Eds.), Dispersal Ecology and Evolution. Oxford University Press, Oxford, pp. 63–82.

Zera, A.J., Denno, R.F., 1997. Physiology and ecology of dispersal polymorphism in insects. Annu. Rev. Entomol. 42, 207–231.

Zera, A.J., Harshman, L.G., 2001. Physiology of life history trade-offs in animals. Annu. Rev. Ecol. Syst. 32, 95–126.

Zera, A.J., Harshman, L.G., 2011. Intermediary metabolism and the biochemical-molecular basis of life history variation and trade-offs in two insect models. In: Flatt, T., Heyland, A. (Eds.), Mechanisms of Life History Evolution. Oxford University Press, Oxford, pp. 311–328.

Zera, A.J., Larsen, A., 2001. The metabolic basis of life history variation: Genetic and phenotypic differences in lipid reserves among life history morphs of the wing-polymorphic cricket, *Gryllus firmus*. J. Insect Physiol. 47, 1147–1160.

Zera, A.J., Mole, S., Rokke, K., 1994. Lipid, carbohydrate and nitrogen content of long- and short-winged *Gryllus firmus*: implications for the physiological cost of flight capability. J. Insect Physiol. 40, 1037–1044.

Zera, A.J., Zhao, Z., 2003. Life-history evolution and the microevolution of intermediary metabolism: activities of lipid-metabolizing enzymes in life-history morphs of a wing-dimorphic cricket. Evolution 57, 568–596.

Zera, A.J., Zhao, Z., 2006. Intermediary metabolism and life-history trade-offs: differential metabolism of amino acids underlies the dispersal-reproduction trade-off in a wing-polymorphic cricket. Am. Nat. 167, 889–900.

Zhao, Z., Zera, A.J., 2001. Enzymological and radiotracer studies of lipid metabolism in the flight-capable and flightless morphs of the wing-polymorphic cricket, *Gryllus firmus*. J. Insect Physiol. 47, 1337–1347.

Zhao, Z., Zera, A.J., 2002. Differential lipid biosynthesis underlies a tradeoff between reproduction and flight capability in a wing-polymorphic cricket. Proc. Natl. Acad. Sci. U.S.A. 99, 16829–16834.

Ziegler, R., 1997. Lipid synthesis by ovaries and fat body of *Aedes aegypti* (Diptera: Culicidae). Eur. J. Entomol. 94, 385–391.